American Mineralogist, Volume 81, pages 743–753, 1996

Hyttsjöite, a new, complex layered plumbosilicate with unique tetrahedral sheets from Långban, Sweden

EDWARD S. GREW,[1] DONALD R. PEACOR,[2] ROLAND C. ROUSE,[2] MARTIN G. YATES,[1] SHU-CHUN SU,[3] AND NICHOLAS MARQUEZ[4]

[1]Department of Geological Sciences, University of Maine, 5711 Boardman Hall, Orono, Maine 04469, U.S.A.
[2]Department of Geological Sciences, University of Michigan, Ann Arbor, Michigan 48109-1063, U.S.A.
[3]Hercules Inc. Research Center, Wilmington, Delaware 19894, U.S.A.
[4]Aerospace Corporation, Los Angeles, California 90009, U.S.A.

ABSTRACT

Hyttsjöite, circa $Pb_{18}Ba_2Ca_5Mn^{2+}_2Fe^{3+}_2Si_{30}O_{90}Cl \cdot 6H_2O$, is a new mineral from the Långban mines, Filipstad district, Värmland, Sweden. It occurs sparingly in Mn-rich skarn with andradite, hedyphane, aegirine, rhodonite, melanotekite, calcite, quartz, potassium feldspar, pectolite, and barite. It is inferred to have formed below 300 °C at 2–4 kbar from the breakdown of medium-temperature metamorphic assemblages in which hedyphane was the principal reactant. The name is from Hyttsjön, which is a lake situated west of the Långban mines. The average analysis is SiO_2 26.38, Al_2O_3 0.02, Fe_2O_3 2.77, CaO 4.35, MnO 2.00, PbO 58.13, BaO 4.65, Cl 0.65, H_2O (calc) 1.58, O = Cl −0.15, total 100.40 wt%. Hyttsjöite grains are mostly 0.1–0.6 mm across, subequant to skeletal in outline, and colorless, and they have a prominent {001} cleavage. Optically, the mineral is uniaxial (−), $\omega = 1.845(4)$, $\epsilon \approx 1.815$. It is trigonal, space group $R\bar{3}$, $a = 9.865(2)$, $c = 79.45(1)$ Å, $V = 6695(3)$ Å^3, and $Z = 3$; $D_{calc} = 5.10$ g/cm^3. The most intense X-ray (Fe$K\alpha$ $\lambda = 1.9373$ Å) powder diffraction lines are as follows [d(Å)(I)(hkl)]: 13.4(50)(006), 4.43(30)(0.0.18), 3.98(30)(027,1.1.12), 3.32(100)(1.0.22,0.0.24,1.1.18), 3.11(40)(217,128), 2.969(40)(2.1.10,0.2.19,1.0.25,1.2.11,0.0.27), and 2.671(80)(1.0.28,2.0.23,1.2.17). The crystal structure consists of composite SiO_4 + PbO_n layers of two kinds (L1 and L2), which are supported by column segments parallel to c, the columns being composed of face-sharing CaO_9, FeO_6, BaO_{12}, and MnO_6 polyhedra. Each layer has two sheets of SiO_4 tetrahedra in pinwheel-like modules, joined together to form a puckered planar network filled out by PbO_n groups. Layer L1 is continuous (Si_8O_{23}), with intralayer Mn, whereas L2 is discontinuous (Si_7O_{22}), with intralayer Fe and Ca. L1 and L2 are distinct from layers in other layered silicates, although they show some similarities to layers in minerals of the gyrolite group.

INTRODUCTION

Study by electron microprobe analysis of a thin section containing some exotic minerals from the Långban mines, Filipstad district, Värmland, Sweden, indicated the presence of a lead silicate of unusual composition. The lattice parameters ($a = 9.865$, $c = 79.45$ Å) measured during the initial stages of characterization of this mineral implied that the structure could be closely related to those of either the gyrolite group of layered silicates (Merlino 1988) or the layered lead silicates jagoite (Mellini and Merlino 1981) and wickenburgite (Lam et al. 1994). These structures are all trigonal or hexagonal, or nearly so, with $a \simeq 9.7$ Å or $\sqrt{3}/2 \times 9.7$ Å (as in jagoite and wickenburgite). The structures of the gyrolite group (e.g., gyrolite, reyerite, and minehillite) all contain layers consisting of single or double tetrahedral sheets and are distinctive in representing articulation of tetrahedral sheets to brucite-like sheets of CaO_6 octahedra. Common layered silicates have tetrahedral sheets articulated to sheets of octahedrally coordinated small cations like Mg^{2+}, Fe^{3+}, and Al^{3+}, whereas modulated layered silicates have tetrahedral sheets articulated to sheets of cations of intermediate radius such as Fe^{2+} and Mn^{2+}. The presence of the large Pb cation, which forms polyhedra characterized by the lone-pair effect, suggested the possibility of structure relations that would extend the structural scheme of the gyrolite group. For that reason, and because the composition initially appeared to be so complex that a crystal-structure analysis was necessary for full characterization, we determined the structure of this extraordinary mineral.

The crystal-structure determination and chemical data showed that the mineral is a new species, which we have named hyttsjöite, with the idealized chemical formula $Pb_{18}Ba_2Ca_5Mn^{2+}_2Fe^{3+}_2Si_{30}O_{90}Cl \cdot 6H_2O$. The name is from Hyttsjön (Swedish *hytta* means smelter, *sjö* means lake, and *n* is the definite article), which is a lake situated just west of the Långban mines. We recommend the pronun-

0003–004X/96/0506–0743$05.00

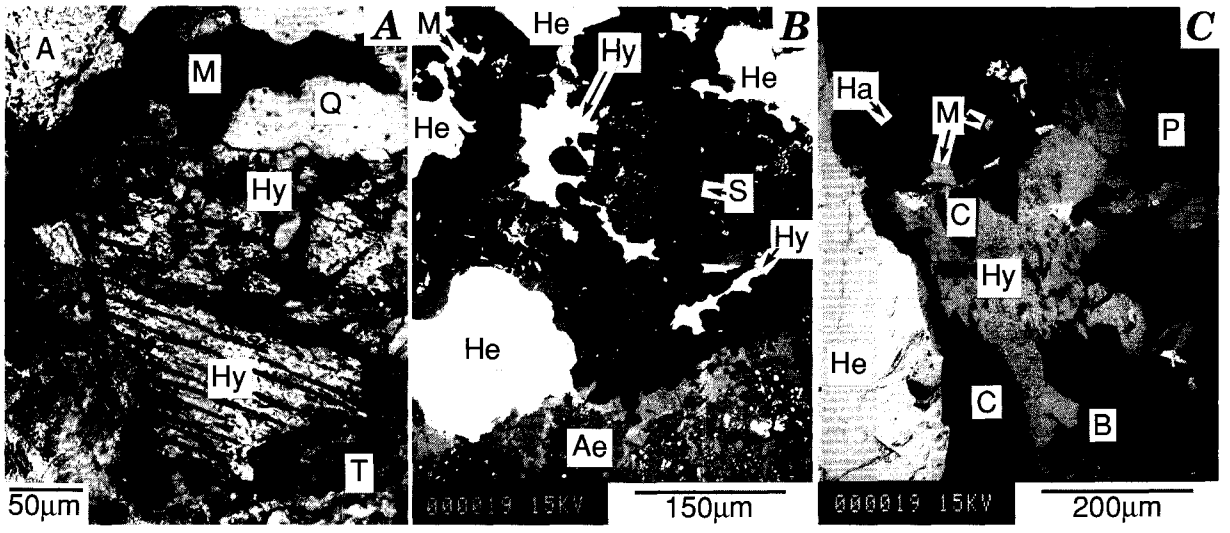

FIGURE 1. (A) Specimen g14913. Plane-light photomicrograph of hyttsjöite (Hy) with quartz (Q), melanotekite (M), andradite (A), and a mixture of a mineral resembling talc with unidentified phases (T). (B) Specimen g14913. Back-scattered electron image of hyttsjöite (Hy, white, skeletal) in a matrix consisting largely of calcite (medium gray, prominent cleavage) and quartz (nearly black, rounded). A mineral resembling stilpnomelane (S, gray like calcite) occurs next to potassium feldspar (dark gray). Hedyphane (He) and minor melanotekite (M) surround the hyttsjöite. Ae represents an aggregate of dominant aegirine (medium gray), subordinant rhodonite (light gray), and hematite (white). (C) Specimen g14915. Back-scattered electron image of hyttsjöite (Hy) adjacent to hedyphane (He) in a matrix of calcite (C), pectolite (P), and barite (B). Other minerals include melanotekite enclosed in pectolite (two grains next to M), a calcium-lead silicate (light gray), and a calcium-barium-lead silicate, possibly hyalotekite (Ha, dark gray).

ciation *hit-show-ite* even though it is an approximation. The new mineral and the name have been approved by the Commission on New Minerals and Mineral Names of the International Mineralogical Association. Holotype material is preserved in the Swedish Museum of Natural History as specimen no. g14913 (under the name hyttsjöite).

Occurrence

Hyttsjöite was found in two museum specimens of hyalotekite-bearing Mn-rich skarn from the Långban mines (Swedish Museum of Natural History nos. g14913 and g14915, Grew et al. 1994). The skarns are dark-colored rocks rich in aegirine, andradite, calcite, and hematite in which hyalotekite occurs as light-gray masses up to several centimeters across. The mineralogical and geochemical relations at Långban and related deposits in the Filipstad area were reviewed by Moore (1970); more recent information is given in Holtstam and Norrestam's (1993) description of the lead ferrite lindqvistite.

Hyttsjöite occurs sparsely; only six grains were positively identified by optical techniques in two thin sections of sample g14913 and two grains in one section of sample g14915. Hyttsjöite grains are mostly 0.1–0.6 mm across and subequant to skeletal in outline (Fig. 1). They were found mostly within 50 μm of large andradite or hedyphane grains, or aegirine ± rhodonite aggregates. Minerals in immediate contact with hyttsjöite are hedyphane, calcite, melanotekite, quartz, potassium feldspar, pectolite, barite, and minerals resembling stilpnomelane and talc, the latter in a finely fibrous aggregate mixed with unidentified phases. Other minerals found in these two specimens are barylite, taramellite (g14913 only), an apophyllite-group mineral, and minerals resembling ecdemite and nadorite (g14915 only) (Grew et al. 1994).

Semiquantitative EDS analyses gave $Mn_{1.64}Ca_{0.33}Si_2O_6$ for rhodonite near hyttsjöite in sample g14913, 12.9–13.5 wt% MnO or X_{Mn} = atomic Mn/(Mn + Ca) = 0.32–0.34 for pectolite contiguous with hyttsjöite in g14913, and 0.8–9.1 wt% MnO or X_{Mn} = 0.02–0.22 for pectolite contiguous with or near hyttsjöite in sample g14915. In general, calcite is barian and manganoan, andradite is calderitic, and hedyphane is barian (Grew et al. 1994).

Petrogenesis

Grew et al. (1994) suggested that hyttsjöite is a late mineral formed during a third, low-temperature event that followed medium-grade metamorphism during two earlier events at temperatures near 500–600 °C and pressures near 2–4 kbar. The textural relations illustrated in Figure 1 show that hyttsjöite could have formed from the breakdown of the medium-temperature assemblages andradite + aegirine + hedyphane ± rhodonite ± taramellite (g14913) and hedyphane + calcite (g14915). The

presence of hedyphane, by virtue of its high contents of Pb, Ba, and Cl, appears to be critical. Associations for hyttsjöite inferred from mutual contacts are hyttsjöite + melanotekite + calcite + pectolite + barite + hedyphane (g14915, Fig. 1C), hyttsjöite + melanotekite + calcite + pectolite + quartz + aegirine + hedyphane (g14913), hyttsjöite + melanotekite + calcite + quartz + potassium feldspar (+ stilpnomelane-like mineral) + aegirine + rhodonite + hedyphane (g14913, Fig. 1B), and hyttsjöite + melanotekite + quartz + andradite (+ talc-like mineral) (g14913, Fig. 1A). The absence of a hyttsjöite + hematite association is noteworthy. In the relatively hematite-rich specimen g14913, hematite is enclosed in aegirine and isolated from hyttsjöite (Fig. 1B). Whether the above-listed associations represent equilibrium is much less clear; the assemblage hyttsjöite + melanotekite + calcite + pectolite ± quartz is present in both samples and may be an equilibrium assemblage.

There are few constraints on the temperature of the third event at Långban, although it very likely did not exceed 300 °C. Pressures probably did not exceed the 2–4 kbar range inferred for the earlier events. Stability ranges for potential index minerals present in samples g14913 and g14915, such as pectolite and minerals of the apophyllite group, have not been studied in detail. Another potential index mineral is cymrite, which occurs with melanotekite, hyalophane, banalsite, hedyphane, and manganophyllite at Långban (Adolfsson 1979) and probably formed as a hydrothermal alteration of celsian at low temperatures (B. Lindqvist, 1994, personal communication). That is, cymrite and hyttsjöite could have formed coevally under identical P-T conditions but in different bulk compositions, hyttsjöite being restricted to rocks depleted in Al. Of the three recent experimental studies of the reaction cymrite = celsian + water (Nitsch 1980; Graham et al. 1992; Hsu 1994), only Hsu's is consistent with a low-pressure stability field for cymrite: $T < 300$ °C at $P = 0.5$–3.0 kbar. Hyttsjöite, like cymrite, contains H_2O molecules, and thus its formation at $T <$ 300 °C is not surprising. In addition, f_{O_2} was sufficiently high for all Fe to be ferric and all S to be sulfate, whereas CO_2 and SO_3 activities were sufficiently low so that no lead, calcium, manganese, or barium carbonate or sulfate appeared with hyttsjöite other than calcite and barite.

Hyttsjöite and hyalotekite are unique among the calcium-iron-manganese-lead silicates reported from Långban (jagoite, ganomalite, nasonite, melanotekite-kentrolite, margarosanite, and barysilite; Flink 1923; Magnusson 1930; Blix et al. 1957) in containing Ba and having Si ≥ other cations. Hyttsjöite is the only lead silicate at Långban that contains substantial H_2O; the others are anhydrous or nearly so, except possibly for jagoite, in which the presence of OH has not been definitively demonstrated (Mellini and Merlino 1981). Thus, hyttsjöite, like hyalotekite, would be expected to occur in relatively silica-rich skarns in which the amount of Ba exceeds that bound up with sulfate in barite, but unlike hyalotekite, hyttsjöite would occur only as a late, hydrothermal mineral in those skarns.

Physical and optical properties

Hyttsjöite has a good {001} cleavage (Fig. 1). It is transparent, colorless, and nonpleochroic in thin section. The luster is adamantine. Hardness could not be accurately determined owing to the minute size of the crystals, and the streak is assumed to be white because the mineral is colorless. The calculated density for the idealized chemical formula is 5.10 g/cm³.

Optically, hyttsjöite is uniaxial negative, with $\omega = 1.845(4)$ on a grain from sample g14913; ϵ was estimated to be 1.815 from the maximum birefringence of 0.03 observed in thin sections of both samples. Calculation of the Gladstone-Dale relationship yields a compatibility index of 0.015, which is in the superior category (Mandarino 1981).

Chemical composition

Hyttsjöite (and jagoite for comparison) were analyzed using a MAC 400s wavelength-dispersive electron microprobe at the University of Maine and an ARL ion microprobe mass analyzer (IMMA) at the Aerospace Corporation (hyttsjöite only). Operating conditions for the MAC 400s microprobe were 15 kV and a sample current of 40 nA on quartz, and the data were reduced with a ZAF correction scheme. The following standards were used: NBS K-456 Pb glass containing SiO_2 28.60, PbO 70.14 wt% (Si$K\alpha$, Pb$M\alpha$), hematite (Fe$K\alpha$), spessartine (Mn$K\alpha$), diopside (Ca$K\alpha$), barite (Ba$L\alpha$), and scapolite (Cl$K\alpha$). Operating conditions for the IMMA were 20 kV and 2.5 nA using a $^{16}O^-$ beam. Ion count ratios were calibrated using data from the following standards: spodumene (Li), surinamite (Al, Be), grandidierite (B), and biotite (F) (Grew et al. 1990). The intensities of peaks for Na, Mg, Al, K, and Ti in hyttsjöite did not significantly exceed background for electron microprobe data. As a result, the maximum possible content of each was estimated from the ion microprobe data, whereas the Al content was semiquantitatively determined using surinamite as a standard.

Initial attempts to specify a chemical formula from the analytical data, taking into account the equipoint ranks of space group $R\bar{3}$ (see below), indicated that crystal-structure data were needed to deduce a formula for hyttsjöite. The formula resulting from the structure analysis ($\sim Pb_{18}Ba_2^{2+}Ca_5Mn_2Fe_2^{3+}Si_{30}O_{90}Cl \cdot 6H_2O$) is compatible with the analytical data, i.e., agreement between this idealized composition and the average of the six electron microprobe analyses is within one estimated standard deviation (esd) for SiO_2, BaO, MnO, and PbO (Table 1). The high standard deviation for PbO is attributed to the low count rates for Pb$M\alpha$. With the exception of Fe_2O_3 (and, to a lesser extent, MnO), the six analyzed grains are uniform in composition. The valence states of Fe^{3+} and Mn^{2+} inferred from crystal-structure relations and overall charge-balance requirements are compatible with the dominant valence states of Fe and Mn in minerals associated with hyttsjöite, e.g., aegirine, calderitic andradite, and manganoan pectolite. In summary, the microprobe

TABLE 1. Chemical analyses of hyttsjöite and jagoite

	Hyttsjöite								
	Idealized	Mean of 6 analyses (esd)	g14913 1	g14913 2	g14913 3	g14913 4	g14915 1	g14915 2	Jagoite 440118
				Electron microprobe					
SiO_2	26.34	26.38(0.16)	26.25	26.59	26.32	26.19	26.38	26.55	22.11
Fe_2O_3	2.33	2.77(0.85)	3.34	3.51	3.44	2.91	1.66	1.76	6.43
MnO	2.07	2.00(0.23)	1.75	1.98	2.05	2.26	2.24	1.72	0.94
CaO	4.10	4.35(0.06)	4.42	4.39	4.25	4.33	4.38	4.30	0.40
PbO	58.70	58.13(0.73)	59.40	57.37	58.00	58.51	57.64	57.88	68.00
BaO	4.48	4.65(0.20)	4.64	4.67	4.50	5.03	4.56	4.47	0.00
Cl	0.52	0.65(0.02)	0.64	0.63	0.68	0.67	0.67	0.62	3.21
				Ion microprobe					
Al_2O_3	—	0.02	0.01	—	0.003	—	0.03	0.03	—
MgO	—	0	≤0.01	—	≤0.01	—	≤0.02	≤0.03	—
SrO	—	0.009	0.008	—	0.007	—	0.01	0.01	—
K_2O	—	0	≤0.01	—	≤0.01	—	≤0.01	≤0.01	—
Na_2O	—	0	<0.05	—	<0.05	—	≤0.1	≤0.1	—
Li_2O	—	0.003	0.001	—	0.001	—	0.005	0.004	—
BeO	—	0.005	0.02	—	0	—	0	0	—
B_2O_3	—	0.004	0.006	—	0	—	0.005	0.004	—
F	—	0	0	—	0	—	0	0	—
				Calculated					
H_2O	1.58	1.58	—	—	—	—	—	—	—
−Cl = 0	−0.12	−0.15	−0.14	−0.14	−0.15	−0.15	−0.15	−0.14	−0.72
Total	100.00	100.40	100.34	99.00	99.10	99.75	97.43	97.21	100.50
			Formula assuming Si + Al + Be + B = 30 (hyttsjöite) or O = 85 (jagoite)						
O equiv.	90	90.58	91.62	91.16	91.40	91.57	89.25	88.63	85
Si	30	29.955	29.920	30.000	29.996	30.000	29.950	29.952	26.436
Be	—	0.014	0.055	—	0	—	0	0	—
B	—	0.007	0.012	—	0	—	0.010	0.008	—
Al	—	0.024	0.013	—	0.004	—	0.040	0.040	—
Fe^{3+}	—	0	0	0	0	0	0	0	3.564
Sum IV	30	30.000	30.000	30.000	30.000	30.000	30.000	30.000	30.000
Fe^{3+}	2	2.367	2.865	2.980	2.950	2.508	1.418	1.494	2.221
Mn	2	1.924	1.689	1.892	1.979	2.193	2.154	1.644	0.952
Li	—	0.013	0.005	—	0.005	—	0.023	0.018	—
Sr	—	0.006	0.005	—	0.005	—	0.007	0.007	—
Ca	5	5.286	5.398	5.307	5.190	5.314	5.328	5.197	0.512
Sum	9	9.596	9.962	10.179	10.129	10.015	8.930	8.360	3.685
K	—	0	0	—	0	—	0	0	0.198
Ba	2	2.067	2.072	2.065	2.010	2.258	2.029	1.976	0
Pb	18	17.770	18.226	17.424	17.794	18.042	17.616	17.578	21.887
Total cations	59	59.433	60.260	59.668	59.933	60.315	58.575	57.914	55.770
Cl	1	1.254	1.236	1.205	1.313	1.301	1.289	1.185	6.505
H_2O	6	6	—	—	—	—	—	—	—

Note: For hyttsjöite, TiO_2 is estimated to be <0.1 wt% from ion microprobe data. For jagoite, the electron microprobe gave K_2O 0.13 and MgO 0.51 wt%; the MgO value is probably not significant. All Fe is assumed to be Fe^{3+}. $\omega \approx 1.89$ for jagoite. Numbers refer to samples from the Swedish Museum of Natural History.

data support the conclusion reached from the crystal-structure analysis that hyttsjöite is a stoichiometric phase with a very limited capacity for cation substitutions. The microprobe data also demonstrate that hyttsjöite is markedly distinct from jagoite, another platy lead-iron-chlorine silicate from Långban (Table 1).

X-RAY CRYSTALLOGRAPHY

Precession and four-circle diffractometer studies of single crystals from sample g14913 showed that hyttsjöite is trigonal, space group $R\bar{3}$, with cell parameters a = 9.865(2), c = 79.45(1) Å, and V = 6695(3) Å^3, for which Z = 3. The lattice parameters were obtained by least-squares refinement from the setting angles of 25 reflections between 12 and 38° 2θ that had been automatically centered by the diffractometer. Powder diffraction data are listed in Table 2.

STRUCTURE SOLUTION AND REFINEMENT

One of three hyttsjöite crystals extracted from thin section was chosen for intensity data measurement, as it was the longest and only crystal to give sharp reflections. Intensity data were measured using an Enraf-Nonius CAD4 diffractometer, and the structure was solved and refined using the Enraf-Nonius crystallographic software system MolEN. Despite the large lattice parameters, all reflections were resolved. Relevant experimental details are summarized in Table 3. Of the 4038 reflections mea-

TABLE 2. Hyttsjöite: X-ray powder diffraction data

I	d_{meas} (Å)	d_{calc} (Å)	hkl
50	13.4	13.2	006
10	8.9	8.8	009
5	7.6	7.5	015
5	6.61	6.62	0.0.12
5	5.89	5.82	1.0.10
5	5.54	5.52	0.1.11
10	5.32	5.30	0.0.15
30	4.43	4.41	0.0.18
5	4.32	4.31	119
		4.29	1.0.16
30	3.98	4.00	027
		3.95	1.1.12
5	3.83	3.78	0.0.21
20	3.68	3.68	2.0.11
5	3.44	3.41	2.0.14
100	3.32	3.33	1.0.22
		3.31	0.0.24
		3.29	1.1.18
40	3.11	3.11	217
		3.07	128
40	2.969	2.991	2.1.10
		2.988	0.2.19
		2.978	1.0.25
		2.947	1.2.11
		2.942	0.0.27
10	2.853	2.877	0.1.26
		2.855	2.1.13
		2.847	030
15	2.759	2.784	036
		2.758	0.2.22
		2.749	1.1.24
80	2.671	2.693	1.0.28
		2.686	2.0.23
		2.656	1.2.17
10	2.574	2.555	2.1.19
5	2.176	2.186	3.1.14
		2.163	1.1.33
10	2.146		
5	2.067		
15	2.019		
15	1.985		
5	1.907		
10	1.873		
20	1.778		

Note: Data obtained using 114.6 mm diameter Gandolfi camera. Fe$K\alpha$ (Ni) radiation. Intensities visually estimated. Data for sample g14913, Swedish Museum of Natural History.

TABLE 3. Experimental details

Crystal size	0.02 × 0.03 × 0.08 mm
Radiation	Monochromatized Mo$K\alpha$
Data measurement:	
Index limits	$0 \le h \le 11$, $0 \le k \le 11$, $-103 \le l \le 103$
Maximum 2θ	54.9°
Scan type	ω-2θ
Scan rates	Between 0 and 7°/min in ω
Scan widths	0.87 + 0.35 tan θ in ω (°)
Intensity monitoring	3 reflections every 3 h
Orientation monitoring	3 reflections every 400 reflections
Data corrections	Lorentz-polarization and absorbtion effects (by the ψ-scan method)
Refinement:	
Type	Full-matrix least-squares
Function minimized	$\Sigma w(\lvert F\rvert_{obs} - \lvert F\rvert_{cal})^2$
Reflection weights	$4F_{obs}^2/\sigma^2(F_{obs}^2)$
Anomalous dispersion	For all atoms
Observations	1198 reflections ($I_{obs} > 3\sigma_I$)
Variables	156 refined parameters
R (observed data)	0.047
R_w (observed data)	0.044
R (all data)	0.311
Esd obs. unit wt.	1.195
Largest shift/error	0.02

sured, 3412 were unique and 1198 of these were considered observed using the criterion $I_{obs} > 3\sigma_I$. Application of the direct-methods program MULTAN11/82, assuming space group $R\bar{3}$, revealed the Pb, Ba, Ca, Fe, and Mn sites, three of the seven Si sites, three of the 18 O sites, and the Cl site. All remaining atoms were located using successive difference electron-density syntheses. Refinement of the structure using isotropic atomic displacement factors converged to an unweighted residual of 0.077. At this point a supplementary absorption correction was applied to the data using the program DIFABS (Walker and Stuart 1983). This supplemental correction was applied because the original absorption correction by the ψ-scan method was considered suspect, owing to the fact that only six reflections, three of which were of low intensity, qualified for use in the ψ-scan procedure. The new correction significantly reduced the residual from 0.077 to 0.051.

The possibility of solid solution on the large cation and Cl sites was tested by placing minor amounts of Ca, Pb, and O on the Pb, Ca, and Cl sites, respectively, and then refining site-occupancy factors. All sites except Pb3 refined to full occupancy by the dominant species within three esds. The refined value for Pb3 was 17.62(7)Pb + 0.38Ca atoms, an apparent degree of solid solution so minor that it was neglected in subsequent calculations. An attempt was also made to refine the structure in the noncentric space group $R3$. This yielded a marginally lower residual (0.046) but also an abundance of negative and large positive values for the isotropic displacement factors. The possibility of $R3$ symmetry was therefore discarded.

Conversion to anisotropic displacement factors for all cations plus Cl reduced the residual from 0.051 to 0.047 but caused the displacement factor of Si7 to become nonpositive definite. Refining the latter atom with an isotropic displacement factor produced the final residuals of 0.047 (unweighted) and 0.044 (weighted) for the 1198 observed reflections and 0.311 for all 3412 reflections. The high value for the latter is ascribed to the predominance of unobserved reflections (65% of the total) in the data set, which, in turn, results from the minute size of the crystal used (Table 3) for intensity measurement. Table 4 contains a list of the observed and calculated structure factors, Table 5 the refined positional and isotropic displacement parameters, Table 6 the anisotropic displacement parameters, and Table 7 selected interatomic distances and angles.[1] Empirical bond-valence sums cal-

[1] A copy of Tables 4 and 6 may be ordered as Document Am-96-615 from the Business Office, Mineralogical Society of America, 1015 Eighteenth Street NW, Suite 601, Washington, DC 20036, U.S.A. Please remit $5.00 in advance for the microfiche.

TABLE 5. Atomic coordinates and isotropic displacement parameters

Atom	x	y	z	U (Å²)
Pb1	0.6784(1)	0.1188(1)	0.64931(2)	0.0156(4)
Pb2	0.0703(1)	0.3986(1)	0.18584(2)	0.0132(4)
Pb3	0.4469(1)	0.0800(1)	0.73591(2)	0.0153(4)
Ba	0	0	0.08632(5)	0.0137(8)
Ca1	0	0	0	0.014(4)
Ca2	0	0	0.7872(2)	0.25(3)
Ca3	0	0	0.8309(2)	0.010(3)
Fe	0	0	0.1306(1)	0.011(1)
Mn	0	0	0.0400(1)	0.015(3)
Si1	0	0	0.4365(2)	0.005(3)
Si2	0.2556(9)	0.3463(10)	0.7260(1)	0.009(3)
Si3	0.3538(9)	0.0862(9)	0.1443(1)	0.011(3)
Si4	0	0	0.6482(2)	0.006(3)
Si5	0.5824(9)	0.5923(9)	0.3082(1)	0.009(3)
Si6	0.5784(9)	0.0034(10)	0.2224(1)	0.010(3)
Si7	0	0	0.2773(2)	0.005(4)*
O1	0.520(3)	0.871(3)	0.4364(3)	0.028(6)*
O2	0.194(2)	0.468(2)	0.7228(3)	0.005(5)*
O3	0.898(2)	0.071(2)	0.4441(3)	0.013(5)*
O4	0.247(2)	0.319(2)	0.1748(3)	0.010(5)*
O5	0.593(2)	0.452(2)	0.2174(3)	0.004(5)*
O6	0.324(2)	0.982(2)	0.2902(3)	0.010(5)*
O7	0.051(2)	0.331(2)	0.3222(3)	0.015(5)*
O8	0.899(2)	0.825(2)	0.2700(3)	0.015(6)*
O9	0.176(2)	0.068(2)	0.3595(3)	0.005(5)*
O10	0.718(2)	0.204(2)	0.1860(3)	0.005(5)*
O11	0.371(3)	0.018(3)	0.1258(4)	0.029(8)*
O12	0	0	0.4168(5)	0.004(8)*
O13	0.192(2)	0.059(2)	0.1898(3)	0.010(5)*
O14	0.856(2)	0.425(2)	0.3118(3)	0.016(6)*
O15	0.626(2)	0.600(2)	0.2588(3)	0.015(6)*
O16	0.663(3)	0.033(3)	0.2395(4)	0.035(8)*
O17	0	0	0.3306(6)	0.02(1)*
O18	0	0	0.2968(5)	0.01(1)*
Cl	0	0	½	0.029(5)*

Note: Estimated standard deviations are in parentheses.
* Refined as isotropic displacement factors. The values shown for the remainder are equivalent isotropic *U*s.

culated using constants of Brese and O'Keeffe (1991) are listed in Table 8.

DESCRIPTION OF CRYSTAL STRUCTURE

Overview

The crystal structure is dominated by two kinds of layers of linked SiO_4 tetrahedra, neither of which has been reported to occur in other layered silicates. These sheets are actually compound, each consisting of two Si-Pb sheets bonded together and enclosing the intralayer cations Fe, Mn, and Ca2 (Table 9). Figure 2 shows four layers from $z = 0$ to ⅓. The first layer, L1, is continuous in that clusters of Si-O tetrahedra are linked to one another (see below), whereas the second, L2, is discontinuous because the clusters of Si-O tetrahedra are isolated. The third and fourth layers are related to L2 and L1, respectively, by inversion centers at $z = \frac{1}{6}$. Alternatively, L1 and L2 can be visualized as plumbosilicate layers because the Si-O tetrahedral nets are filled out by PbO_n polyhedra. The z coordinates of Pb and Si differ by no more than 0.01 in a given plane (Table 9), i.e., Pb and Si are virtually coplanar. On the other hand, in the intralayer region, oc-

TABLE 7. Selected interatomic distances (Å) and angles (°)

Pb1-O7	2.36(2)	Pb2-O13	2.28(2)
Pb1-O7	2.46(3)	Pb2-O4	2.34(2)
Pb1-O17	2.47(2)	Pb2-O4	2.40(2)
Pb1-O18	2.66(3)	Pb2-O10	3.01(2)
Pb1-O9	2.93(2)	Pb2-Cl	3.030(2)
Pb1-O14	3.10(2)	Pb2-O11	3.23(3)
Pb1-O7	3.15(2)	Pb2-O3	3.25(3)
Pb1-O6	3.38(2)	Pb2-O5	3.29(2)
Mean	2.81	Mean	2.83
Pb3-O16	2.24(3)	Ba-O5	2.88(2) × 3
Pb3-O15	2.26(2)	Ba-O2	2.96(2) × 3
Pb3-O2	2.59(2)	Ba-O15	3.00(2) × 3
Pb3-O12	2.61(2)	Ba-O16	3.01(3) × 3
Pb3-O8	3.23(2)	Mean	2.96
Pb3-O6	3.35(2)		
Mean	2.71		
Ca1-O14	2.35(3) × 6	Ca2-O1	2.38(3) × 3
Mean	2.35	Ca2-O13	2.49(3) × 3
		Ca2-O11	3.05(3) × 3
Ca3-O13	2.35(3) × 3	Mean	2.64
Ca3-O10	2.36(3) × 3		
Ca3-O4	2.90(2) × 3		
Mean	2.54		
Fe-O5	2.02(2) × 3	Mn-O2	2.16(2) × 3
Fe-O10	2.08(2) × 3	Mn-O14	2.19(3) × 3
Mean	2.05	Mean	2.18
Si1-O12	1.56(5)	O3-Si1-O3	107(1) × 3
Si1-O3	1.61(3) × 3	O3-Si1-O12	112(1) × 3
Mean	1.60	Mean	109
Si2-O15	1.58(3)	O2-Si2-O8	107(1)
Si2-O2	1.62(2)	O6-Si2-O8	107(1)
Si2-O6	1.62(3)	O6-Si2-O15	108(1)
Si2-O8	1.64(3)	O8-Si2-O15	110(2)
Mean	1.61	O2-Si2-O15	111(1)
		O2-Si2-O6	113(1)
		Mean	109
Si3-O10	1.58(2)	O11-Si3-O13	105(1)
Si3-O13	1.63(2)	O4-Si3-O11	107(1)
Si3-O4	1.63(3)	O4-Si3-O13	107(1)
Si3-O11	1.66(3)	O10-Si3-O13	110(1)
Mean	1.62	O10-Si3-O11	111(1)
		O4-Si3-O10	115(1)
		Mean	109
Si4-O9	1.63(2) × 3	O9-Si4-O9	107(1) × 3
Si4-O17	1.69(5)	O9-Si4-O17	112(1) × 3
Mean	1.64	Mean	109
Si5-O7	1.57(3)	O6-Si5-O9	104(1)
Si5-O14	1.58(3)	O6-Si5-O7	106(1)
Si5-O6	1.63(3)	O7-Si5-O9	107(1)
Si5-O9	1.65(2)	O9-Si5-O14	108(1)
Mean	1.61	O7-Si5-O14	114(2)
		O6-Si5-O14	117(1)
		Mean	109
Si6-O16	1.54(3)	O3-Si6-O5	107(1)
Si6-O5	1.58(2)	O3-Si6-O11	107(1)
Si6-O3	1.67(3)	O11-Si6-O16	109(2)
Si6-O11	1.67(3)	O5-Si6-O11	110(1)
Mean	1.61	O3-Si6-O16	112(2)
		O5-Si6-O16	112(2)
		Mean	109
Si7-O18	1.55(5)	O8-Si7-O8	108(1) × 3
Si7-O8	1.60(3) × 3	O8-Si7-O18	111(1) × 3
Mean	1.59	Mean	109
Si1-Si6	3.04(1) × 3	Si1-O3-Si6	136(2) × 3
Si2-Si5	3.06(2)	Si2-O6-Si5	140(2)
Si2-Si7	3.08(1)	Si2-O8-Si7	143(2)
Si3-Si6	3.05(2)	Si3-O11-Si6	133(2)
Si4-Si5	2.94(1) × 3	Si4-O9-Si5	127(1) × 3
Si5-Si4	2.94(1)	Si5-O9-Si4	127(1)
Si5-Si2	3.06(2)	Si5-O6-Si2	140(2)
Si6-Si1	3.04(1)	Si6-O3-Si1	136(2)
Si6-Si3	3.05(2)	Si6-O11-Si3	133(2)
Si7-Si2	3.08(1) × 3	Si7-O8-Si2	143(2) × 3
Mean	3.03	Mean	136

Note: Mean bond length for Pb2 is for Pb-O bonds only. Estimated standard deviations are in parentheses.

TABLE 8. Empirical bond-valence sums (vu)

Pb1	1.8	Si1	4.3	O3	2.0	O12	2.0
Pb2	2.1	Si2	4.1	O4	2.1	O13	2.2
Pb3	2.0	Si3	4.0	O5	1.9	O14	1.9
Ba	2.0	Si4	3.8	O6	2.1	O15	1.9
Ca1	2.1	Si5	4.2	O7	2.1	O16	2.1
Ca2	1.9	Si6	4.2	O8	2.1	O17	2.0
Ca3	2.3	Si7	4.4	O9	2.0	O18	1.9
Fe	2.8	O1	0.3	O10	2.0	Cl	1.6
Mn	2.1	O2	1.8	O11	1.9		

TABLE 9. Sequence of planes of atoms along *c*

No. of layer/ interlayer	Ideal *z* of center of layer/interlayer	Cation, Cl, and H_2O sites (refined *z* values)
I1	0/24(0.0000)	Ca1(0)
[L1]	1/24(0.0417)	Si4(0.019), Si5(0.025), Pb1(0.018) Mn(0.040) Si2(0.059), Si7(0.056), Pb3(0.069)
I2	2/24(0.0833)	Ba(0.086)
[L2]	3/24(0.1250)	Si1(0.103), Si6(0.111), H_2O(0.103) Fe(0.131), Ca2(0.120) Si3(0.144), Pb2(0.147)
I3	4/24(0.1667)	Ca3(0.164, 0.169), Cl(1/6)
[L3] [L2]	5/24(0.2083)	Si3(0.189), Pb2(0.186) Fe(0.202), Ca2(0.213) Si1(0.231), Si6(0.222), H_2O(0.231)
I4 I2	6/24(0.2500)	Ba(0.246)
[L4] [L1]	7/24(0.2917)	Si2(0.274), Si7(0.277), Pb3(0.264) Mn(0.293) Si4(0.315), Si5(0.308), Pb1(0.316)
I5 [I1]	8/24(0.3333)	Ca1(1/3)

tahedrally coordinated Mn and Fe, or Ca2 in a 6 + 3 coordination, have *z* coordinates intermediate between those of Si and Pb in adjacent sheets and thus serve further to bind two sheets together to form layers.

Ca1, Ba, and Ca3 are interlayer cations that are located between L1, L2, and their inversion-related equivalent sheets, and this accentuates the layered nature of the hyttsjöite structure (Table 9). The interlayer cations are widely dispersed, and their coordination polyhedra do not share edges or vertices within a given (001) sheet. However, these interlayer cations, in conjunction with the intralayer cations Mn, Fe, and Ca2, form column segments of face-sharing coordination polyhedra parallel to *c* (Fig. 3). The coordinates of all intralayer cations (which define the centers of the layers L1, L2, etc.) and all interlayer cations (which define I1, I2, etc.) are nearly multiples of $\frac{1}{24}c$, hence the designation "ideal *z*" in Table 9.

Plumbosilicate layers

The basic structural units in L1 and L2 are two, nearly identical pinwheel-like modules, each composed of four tetrahedra (Figs. 4 and 5). In L1, one module is centered on Si7, which is on a threefold axis, with three Si2 tetrahedra as pinwheel wings (Fig. 4). The other module is centered on Si4, which is also on a threefold axis, with three Si5 tetrahedral wings. Si2 and Si5 tetrahedra share a vertex, thereby linking the pinwheels into a continuous network with an Si:O ratio of Si_8O_{23}. Alternatively, the pinwheel of tetrahedra around Si7 can be visualized as having wings composed of two tetrahedra (Si2 and Si5), these pinwheels being linked by Si4, a method of view more suitable for comparison with layer L2 (see below). Because the Si7-Si2 and Si4-Si5 pinwheels are centered at different levels, i.e., at $z = 0.06$ and 0.02, respectively, the planar Si-O network appears to be puckered.

In layer L2, the lone pinwheel-like module is centered on Si1, which is on a threefold axis, with three pairs of Si6 + Si3 tetrahedra as pinwheel wings (Fig. 5). Thus, Si1 is equivalent in its structural role to Si7 in L1. The equivalent of the cross-linking Si4 is absent, and, consequently, the pinwheels are insular. This produces an Si:O ratio of Si_7O_{22} for L2. The missing tetrahedron lies within the volume occupied by the polyhedron around the intralayer cation Ca2, which has a 6 (+3) coordination.

In layer L1, the intralayer cation Mn is situated midway between the upper sheet of tetrahedron (Si2 + Si7) and the lower sheet (Si4 + Si5). It shares three vertices each with Si2 and Si5 tetrahedra, thereby defining an octahedron with two faces normal to *c*. In layer L2, the intralayer cation Fe shares vertices with Si3 and Si6, resulting in octahedral coordination analogous to that of Mn in L1.

In summary, layers L1 and L2 are topologically similar, with Mn and Si4 of L1 being equivalent, respectively, to Fe and Ca2 of L2. The topological identity of adjacent L1 and L2 layers becomes apparent with a 60° rotation of L1 relative to L2. However, the disposition of Pb in L1 and L2 is different, so that the topological equivalence is limited to the Si-O network and the intralayer Mn, Fe, and Ca2 cations.

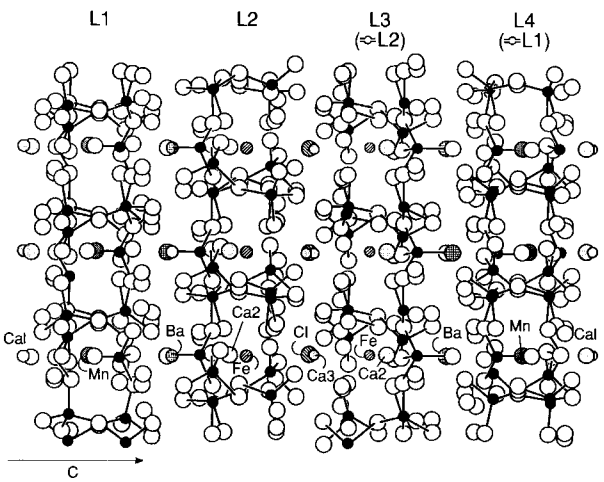

FIGURE 2. An edge view (perpendicular to *c*) of four plumbosilicate layers from $z = 0$ to $\frac{1}{3}$, showing the positions of the intralayer cations (Mn, Fe, Ca2) and the interlayer cations (Ca1, Ca3, Ba). The sheets, from left to right, are of types L1, L2, L2, and L1.

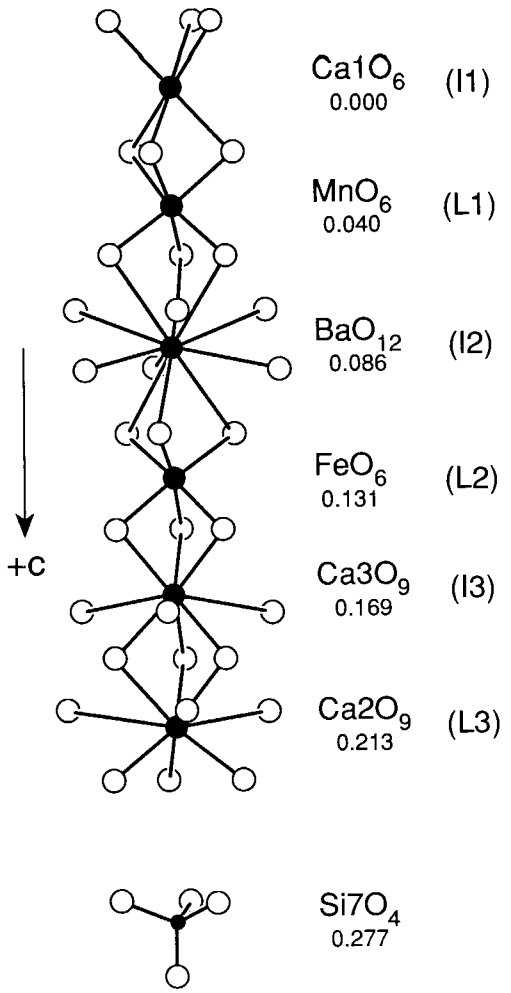

FIGURE 3. Column segment of face-sharing polyhedra. Only one-half of the column segment is shown, the other half being related to that shown by inversion at Ca1.

Relation of tetrahedral layers to those of other layered silicates. During the initial stages of characterization of hyttsjöite, a resemblance was noted between its symmetry and cell parameters and those of the gyrolite group. The latter are hexagonal or trigonal (or nearly so), with a = 9.7 Å and large values of c indicative of complex layered structures, all of which suggests a structural relationship to the new mineral. Indeed, hyttsjöite does have discrete tetrahedral layers, as do members of the gyrolite group. However, the layers in members of the gyrolite group, as exemplified by the gyrolite structure (Merlino 1988), consist of continuous tetrahedral layers, which resemble layers found in common phyllosilicates in that all tetrahedra share three vertices. In structures of the gyrolite group, however, not all tetrahedra have vertices directed only above or below a given sheet, as in micas, for example. That permits tetrahedra of two individual sheets to share vertices to form a layer consisting of two cross-linked sheets.

Because the linkage of tetrahedral layers in hyttsjöite is very different from those in gyrolite-group structures, the question remains as to how the intralayer periodicities (a = 9.7 Å) could be so similar. The answer lies in the pinwheel-like units. Tetrahedral layers in gyrolite-group structures (and those of common phyllosilicates and wickenburgite) may also be viewed as composed of pinwheels consisting of a central tetrahedron with three wings, each wing consisting of a single tetrahedron. If the double tetrahedral wings of layers in hyttsjöite (for which the two tetrahedra are nearly superimposed in the c-axis direction) are replaced by a single tetrahedron, a single gryolite-like layer is formed. The nine-membered rings of hyttsjöite are thus replaced by the familiar six-membered rings of gyrolite-like or common phyllosilicate sheets. Because the double-tetrahedron units of hyttsjöite are nearly superimposed in the c-axis direction, the resulting periodicity in the (001) plane is equivalent to that of gyrolite-group structures.

Pb coordinations and relation to layers of tetrahedra. The Pb coordination polyhedra defined by O and Cl are shown in Figure 6. The polyhedron around Pb3 is a highly distorted octahedron, with upper and lower triangular faces defined by O6-O8-O12 and O2-O15-O16, respectively. The coordinations about Pb1 and Pb2 can be regarded as very distorted square antiprisms (or cubes). More important, each Pb atom has either three or four short bonds in the range 2.3–2.6 Å, all others being 2.9 Å or longer. The short bonds define PbO_3 and PbO_4 pyramids with Pb at the apices, implying that the lone electron pairs of the Pb atom are stereochemically active and are directed opposite to the pyramid bases.

The short Pb-O bonds are all directed to O atoms that are in turn coordinated to Si atoms, i.e., there are Pb-O-Si bridges. However, the short bonds associated with each of the Pb1, Pb2, and Pb3 polyhedra are directed both to O atoms coordinated to Si atoms within the same layer and to O atoms coordinated to Si atoms of adjacent layers. The strongest Pb-O bonds thus serve to bond adjacent tetrahedral layers to one another, and in this sense the combination of Si-O and short Pb-O bonds forms a three-dimensional array despite the obvious layered nature of the structure. However, the Pb-O-Si interlayer bridges are much weaker linkages than the Si-O-Si intralayer bridges, as expressed by the perfect {001} cleavage.

Column segments

All cations except Pb and Si form column segments (Fig. 3) of face-sharing polyhedra oriented parallel to c. The sequence is Ca1-Mn-Ba-Fe-Ca3-Ca2, but this is doubled in length because of the inversion center at Ca1. All the cations reside on a threefold axis, and thus the shared polyhedron faces are triangular and oriented normal to c. Coordinations range from slightly distorted MO_6 octahedra for Mn, Fe, and Ca1 to the moderately distorted BaO_{12} cuboctahedron, the latter being a common coordination for this element. Ca3 has a well-defined, ninefold, tricapped trigonal prismatic coordination (Fig. 7), whereas the exact coordination number of Ca2 is some-

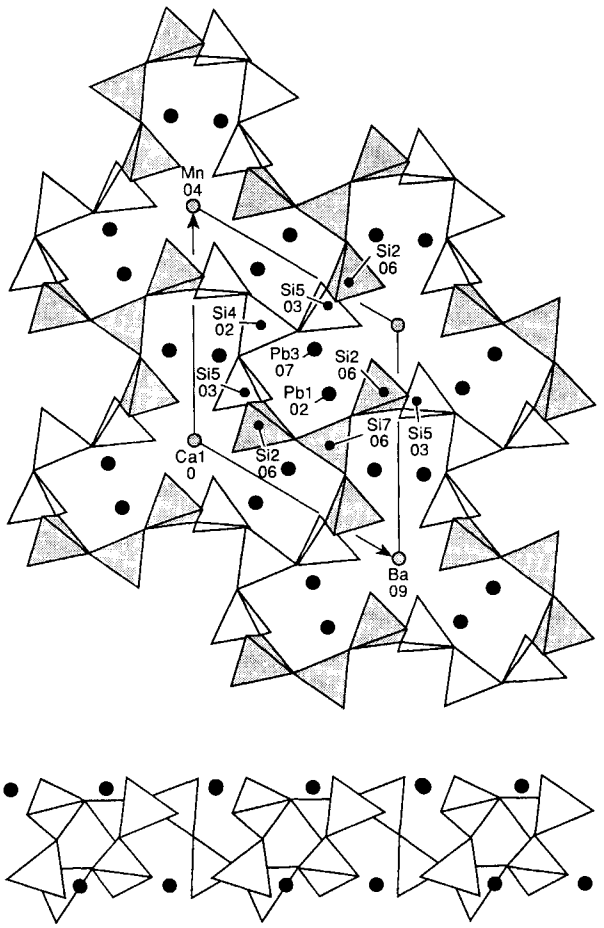

FIGURE 4. (**top**) A projection of silicate layer L1 on (001), showing the tetrahedra and the positions of the Pb atoms (Pb1 and Pb3) associated with L1. Pinwheels centered at the higher level (z = 0.06) are shaded. Numbers below atom labels are z coordinates ×100. (**bottom**) Projection of L1 normal to c.

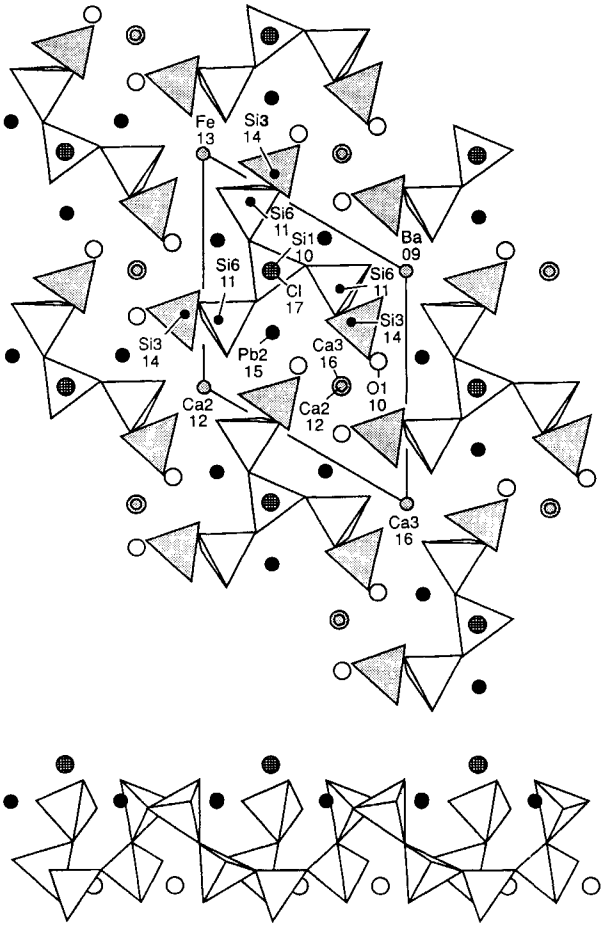

FIGURE 5. (**top**) A projection of silicate layer L2 on (001), showing the tetrahedra and the positions of the Pb atoms (Pb2). The O1 atoms are part of the H_2O molecules. Tetrahedra centered at the higher level (z = 0.14) are shaded. Numbers below atom labels are z coordinates ×100. (**bottom**) Projection of L2 normal to c.

what ambiguous. The polyhedron could be considered a trigonal prism with three upper O atoms, which are also coordinated to Si3, and three lower O atoms that are part of H_2O molecules. If the three long Ca2-O11 distances are also considered to be bonds, the polyhedron becomes a tricapped trigonal prism, $Ca2O_6(H_2O)_3$ (Fig. 7) similar to that around Ca3. The column segments can be viewed as pillars supporting the plumbosilicate sheets, analogous to columns supporting the floors of a building (Fig. 2).

Moore has noted (personal communication) that the structure of hyttsjöite is closely related to those of fillowite and related materials, which Moore (1989) described as based on collections of parallel rods. Moore (personal communication) pointed out that, as with fillowite, the hyttsjöite structure can be viewed as consisting of parallel columns (rods) of polyhedra of two types, which he referred to as type I and type II. These columns have atoms with coordinates (0,0,z) and ($\frac{1}{3}$,$\frac{1}{3}$,z), respectively, as projected onto (001), forming a $\{6_3\}$ net. Moore further noted that the rods can be viewed as consisting of continuous sequences of polyhedra with periodicities of 24 beads (polyhedra), as defined by the occurrence of cations with values of z that are multiples of $\frac{1}{24}$, if vacant sites and tetrahedral sites are included in the sequences of polyhedra. He also noted "that such rod structures (i.e., those of steenstrupine, cerite, and fillowite) derive from cation-dominated structural principles, the anions essentially making up the Pauling polyhedra but of no great architectural consequence." This is an alternative way of viewing the structure, in contrast to the description given above, in which the linear sequences of polyhedra are viewed as consisting only of edge-sharing polyhedra having six or more vertices, i.e., as discontinuous column segments knitting plumbosilicate layers together.

CHEMICAL FORMULA

The chemical analysis of hyttsjöite is so complex that the full chemical formula could not be defined without

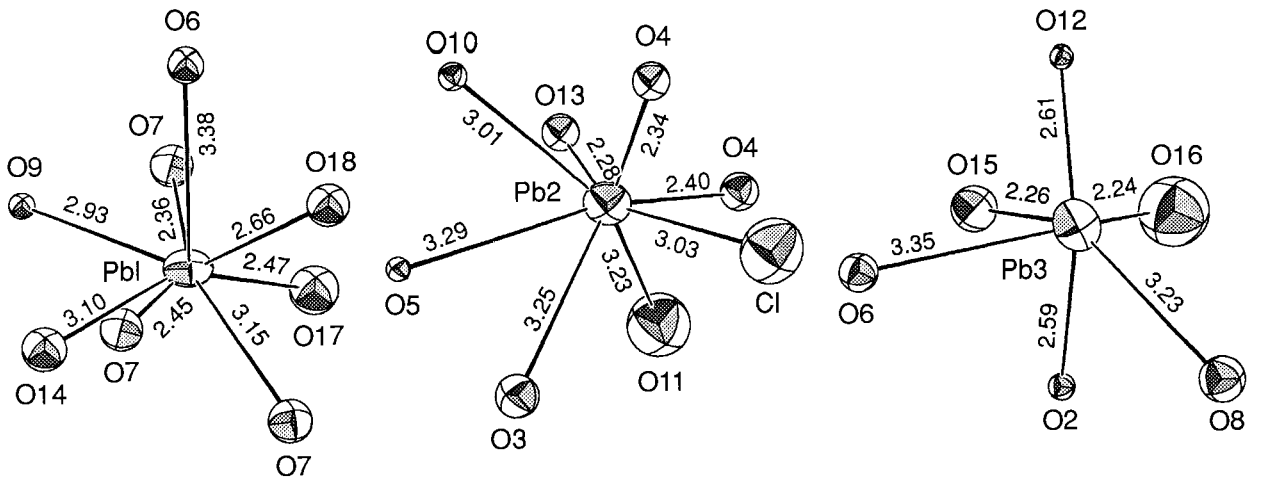

FIGURE 6. The coordinations of each of the three nonequivalent Pb atoms.

data from the crystal-structure analysis. As noted above, the possibility of mutual solid solution of Pb and Ca (and Cl and OH) was tested by refinement of population factors, but the results indicated a lack of significant solid solution. Such solid solution is improbable in any event, given the evident lone-electron-pair activity of the Pb^{2+} ion. Mutual population factors for Mn and Fe could not be refined because of the similarity in scattering factors. We therefore relied largely on interatomic distance to verify occupancies for these atoms. The cuboctahedral coordination polyhedron of Ba is unique to that large atom relative to other atoms in the structure. The mean interatomic distances for the Fe, Mn, and Ba polyhedra (2.05, 2.18, and 2.96 Å, respectively) are compatible with occupancy only by Fe^{3+}, Mn^{2+}, and Ba^{2+}, respectively. The mean Ca-O distances (2.35, 2.64, and 2.54 Å, respectively) and coordination polyhedra geometries are also consistent with occupancy only by Ca. Therefore, even though the crystal structure is exceedingly complex, with many different sites, it seems to be characterized by a lack of any significant solid solution.

The bond-valence sums shown in Table 8 are likewise consistent with valences of 3+ for Fe and 2+ for Mn. Valence sums for all other cations are reasonable. However, the sum for O1 (0.33) clearly indicates that O1 corresponds to H_2O. O1 is bonded to only one atom, Ca2, at a distance of 2.38(3) Å. The valence sum for Cl (1.56) exceeds its ideal value because of the high coordination number of Cl (6 Pb atoms), but the site-occupancy factor refinement yielded 2.3(3) Cl, which is within 2.5 esd of the full-occupancy value of 3. The large standard error, assumed to be a function of the limited intensity data of below-average precision and the dominance of atoms with large X-ray scattering factors, prevents further analysis. The deficiencies in the intensity data set, especially as seen in the large proportion of unobserved intensities, are also inferred to have resulted in some unreasonably short Si-O distances, as shown in Table 7 (i.e., Si1-O12 =

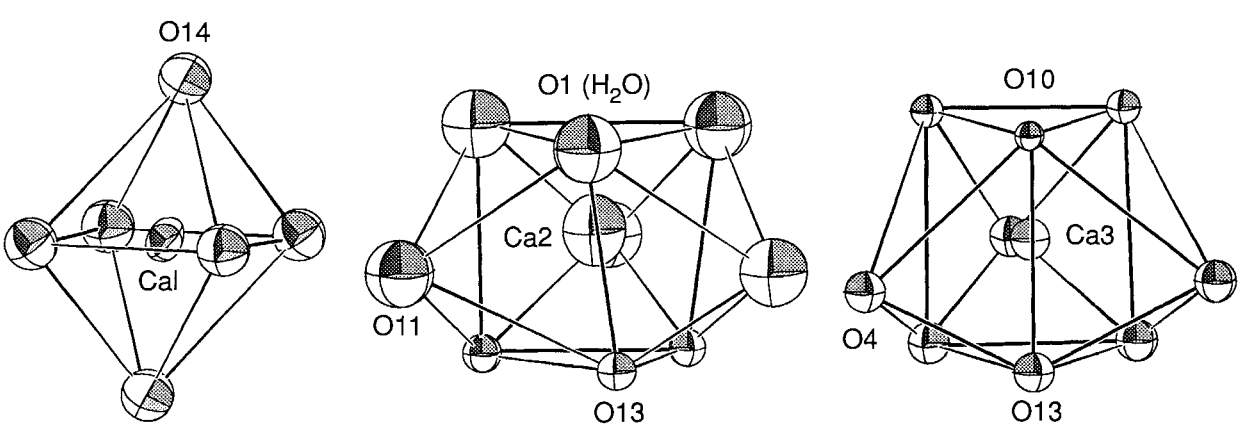

FIGURE 7. The coordination polyhedra around each of the three nonequivalent Ca atoms.

1.56(5), Si7-O18 = 1.55(5), and Si6-O16 = 1.54(3) Å). Note, however, that these differ by no more than one esd from the minimum known Si-O value of 1.57 Å cited by Liebau (1985).

The full formula derived on the basis of the structure analysis is therefore $Pb_{18}Ba_2Ca_5Mn\ {}^{2}_{2}{}^{+}Fe\ {}^{3}_{2}{}^{+}Si_{30}O_{90}Cl\cdot 6H_2O$. Calculations of the weight percents give values in excellent agreement with those of the chemical analysis (Table 1). However, the formula is not balanced: Positive and negative charges sum to +180 and −181 vu, respectively. Attempts to find a source of additional positive charge, including analyses of difference electron-density syntheses and charge balance, were unsuccessful. Only two possibilities, neither supported by any direct evidence, seem reasonable: (1) Substitution of OH for O atoms, presumably for O1 (in H_2O) because all others are bonded to Si. All equipoints occupied by O are of ranks 6 or 18, and the charge deficiency for the full cell contents is +3 (Z = 3). If such substitution were random, the average bond valences would not be noticeably affected for a site of rank 18, as is the case for O1. (2) One-half of Mn^{2+} may actually be Mn^{3+}. The average Mn-O distance, 2.18 Å, is actually approximately 0.04 Å shorter than normal for Mn^{2+}, consistent with partial occupancy by Mn^{3+}, but the bond-valence sum for Mn is 2.13, which is only slightly greater than the ideal value for Mn^{2+}. There is, therefore, some residual uncertainty in the chemical formula of hyttsjöite, despite all the rather complete effort to characterize this chemically and structurally complex species.

Acknowledgments

We thank Bengt Lindqvist of the Swedish Museum of Natural History for specimens g14913, g14915, and 440118, and for the information on cymrite and the interpretation of its paragenesis; James J. McGee for the lead glass standard; and Eleanor Wikborg for assistance with the pronunciation and derivation of the name hyttsjöite. We are grateful for the comments of an anonymous reviewer and those of Paul Moore, especially relative to insights into the relation between the structure of hyttsjöite and those of fillowite and related minerals. This research was supported by U.S. National Science Foundation grant EAR-9118408 to the University of Maine.

References cited

Adolfsson, S.G. (1979) Notes on recent underground collecting at Långban. Mineralogical Record, 10, 215–217.

Blix, R., Gabrielson, O., and Wickman, F.E. (1957) Jagoite, a new lead-silicate mineral from Långban in Sweden. Arkiv för Mineralogi och Geologi, 2, 315–317.

Brese, N.E., and O'Keeffe, M. (1991) Bond-valence parameters for solids. Acta Crystallographica, B47, 192–197.

Flink, G. (1923) Über die Långbansgruben als Mineralvorkommen. Zeitschrift für Kristallographie, 58, 356–385.

Graham, C.M., Tareen, J.A.K., McMillan, P.F., and Lowe, B.M. (1992) An experimental and thermodynamic study of cymrite and celsian stability in the system BaO-Al_2O_3-SiO_2-H_2O. European Journal of Mineralogy, 4, 251–269.

Grew, E.S., Chernosky, J.V., Werding, G., Abraham, K., Marquez, N., and Hinthorne, J.R. (1990) Chemistry of kornerupine and associated minerals, a wet chemical, ion microprobe, and X-ray study emphasizing Li, Be, B and F contents. Journal of Petrology, 31, 1025–1070.

Grew, E.S., Yates, M.G., Belakovskiy, D.I., Rouse, R.C., Su, S.-C., and Marquez, N. (1994) Hyalotekite from reedmergnerite-bearing peralkaline pegmatite, Dara-i-Pioz Tajikistan and from Mn skarn, Långban, Värmland, Sweden: A new look at an old mineral. Mineralogical Magazine, 58, 285–297.

Holtstam, D., and Norrestam, R. (1993) Lindqvistite, $Pb_2MeFe_{16}O_{27}$, a novel hexagonal ferrite mineral from Jakobsberg, Filipstad, Sweden. American Mineralogist, 78, 1304–1312.

Hsu, L.C. (1994) Cymrite: New occurrence and stability. Contributions to Mineralogy and Petrology, 118, 314–320.

Lam, A.E., Groat, L.A., Cooper, M.A., and Hawthorne, F.C. (1994) The crystal structure of wickenburgite, $Pb_3CaAl[AlSi_{10}O_{27}](H_2O)_3$, a sheet structure. Canadian Mineralogist, 32, 525–532.

Liebau, F. (1985) Structural chemistry of silicates, 347 p. Springer-Verlag, Berlin.

Magnusson, N.H. (1930) Långbans Malmtrakt Geologisk Beskrivning. Sveriges Geologiska Undersökning, series Ca, no. 23, 111 p.

Mandarino, J.A. (1981) The Gladstone-Dale relationship: Part IV. The compatibility concept and its application. Canadian Mineralogist, 19, 441–450.

Mellini, M., and Merlino, S. (1981) The crystal structure of jagoite. American Mineralogist, 66, 852–858.

Merlino, S. (1988) Gyrolite: Its crystal structure and crystal chemistry. Mineralogical Magazine, 52, 377–387.

Moore, P.B. (1970) Mineralogy & chemistry of Långban-type deposits in Bergslagen, Sweden. Mineralogical Record, 1, 154–172.

——— (1989) Perception of structural complexity: Fillowite revisited and α-iron related. American Mineralogist, 74, 918–926.

Nitsch, K.-H. (1980) Reaktion von Bariumfeldspat (Celsian) mit H_2O zu Cymrit unter metamorphen Bedingungen. Fortschritte der Mineralogie, 58 (Beiheft 1), 98–100.

Walker, N., and Stuart, D. (1983) An empirical method for correcting diffractometer data for absorption effects. Acta Crystallographica, A39, 158–166.

Manuscript received December 16, 1994
Manuscript accepted January 16, 1996